DOI: 10.26599/FSHW.2026.9251060

Contents lists available at SciOpen

Food Science and Human Wellness

journal homepage: https://www.sciopen.com/journal/2097-0765

China Food Publishing Co.

The complexes of maize starch-chlorogenic acid regulated the blood glucose homeostasis by alleviating insulin resistance

Yuxue Zheng [a], Xiaoning Yu [a], Yanyu Hu [a], Siyu Chen [b], Suwen Liu [c], Xingqian Ye [e], Henry Huang [d], Tingting Liu [d], Shaoyun Wang [a] *, Jinhu Tian [e] *

[a] *College of Biological Science and Engineering, Institute of Food and Marine Bio-Resources, Fuzhou University, Fuzhou 350108*

[b] *Department of Food Science and Technology, National University of Singapore, 2 Science Drive 2, Singapore 117542*

[c] *College of Food Science & Technology, Hebei Normal University of Science and Technology, Qinhuangdao, Hebei 066004, China*

d Fujian Orientland Foods Co., LTD

[e] *College of Biosystems Engineering and Food Science, Zhejiang University, Hangzhou 310058*

ABSTRACT: Our study aimed to explore the ability of extruded maize starch-chlorogenic acid (EMS-CHA) complexes to regulate blood glucose homeostasis. Extrusion processing was used to successfully prepare EMS-CHA complexes, accompanied by a structural transformation of starch from A-type to A+V-type semi-crystalline form. Notably, when chlorogenic acid (CHA) was incorporated at 2.0% (w/w) into maize starch (EMS-2.0CHA), the resistant starch content significantly increased to 30.35 ± 2.36%. This directly contributed to a reduced glycemic response, as evidenced by a lower postprandial blood glucose area under the curve (AUC) of 5.72 ± 1.13 mmol/h·L. The hypoglycemic effect of EMS-2.0CHA complex was further validated in diabetic rats. Compared with high-fat diet group, supplementation with EMS-2.0CHA complex significantly decreased fasting blood glucose levels to 11.75 ± 2.75 mmol/L and reduced the AUC to 15.15 ± 2.63 mmol/h·L. Importantly, these improvements were associated to enhanced pancreatic function: increasing insulin secretion, improving pancreatic mass and reduced apoptosis, thereby ameliorating insulin resistance. These findings initially clarify the mechanism by which dietary extruded maize starch-chlorogenic acid complexes alleviated insulin resistance and provided a better understanding of the influence of chlorogenic acid on starch that promotes body blood glucose homeostasis.

Keywords: maize starch, chlorogenic acid, insulin resistance, blood glucose homeostasis.

1. Introduction

Maintaining blood glucose homeostasis is essential for normal physiological functions [1]. Disruptions of glucose regulation is closely linked to metabolic disorders, including obesity, diabetes, and cardiovascular diseases [2]. In particular, obesity-related type 2 diabetes is characterized by impaired glucose homeostasis s-a condition that can be exacerbated by unhealthy dietary patterns [3]. Conventional pharmacological treatments—such as acarbose, metformin, and pioglitazone-are commonly used to manage blood sugar levels

***Corresponding author**
shywang@fzu.edu.cn (Wang S), jinhutian@126.com (Tian J)

Received 8 October 2025
Received in revised from 14 November 2025
Accepted 3 December 2025

but may induce adverse effects, including hepatotoxicity and gastrointestinal disturbances [4]. In contrast, dietary intervention represents a safer and more sustainable strategy for glycemic control.

Starch, composed of amylose and amylopectin, is the most important carbohydrate in the human diet [5] and can be hydrolyzed into glucose by digestive enzymes and absorbed into bloodstream, then subsequently utilized by the tissue and organs [6]. Normally, starch is typically classified into three categories: rapidly digestible starch (RDS), slowly digestible starch (SDS) and resistant starch (RS). RDS could be hydrolyzed in 20 min and raise the blood glucose immediately [7]. While SDS (hydrolyzed in 20~120 min) and RS (can't be hydrolyzed in the small intestine) have been reported to maintain postprandial blood glucose stability [8]. The beneficial effects of RS on diabetes are mainly mediated by regulating glycemic response, improving insulin sensitivity, suppressing appetite and modulating gut microbiota composition [9]. Thus, modifying starch to increase SDS and RS content represents a promising dietary strategy for optimizing blood glucose homeostasis by delaying starch digestion.

Growing evidence indicates that numerous bioactive phytochemicals can form starch-polyphenol complexes with starch via non-covalent interaction [10]. These complexes modulate starch digestion through multiple mechanisms: (1) inhibiting digestive enzymes (e.g., α-amylase and α-glucosidase), (2) competitively binding to α-1,4/α-1,6 glucoside bonds to block enzymatic hydrolysis, or (3) altering starch structure to reduce enzymatic accessibility [11-13]. Additionally, phytochemicals could also alleviate glucose metabolic dysfunction and its complications (e.g. chlorogenic acid, epigallocatechin gallate, curcumin, resveratrol, and anthocyanins, etc. [14]. However, current research is mostly limited to the monitoring of postprandial blood glucose response-related indicators of starch-polyphenol complexes, as well as their preliminary application and functional characteristic evaluation. It has not been fully expanded to the exploration of the mechanism of regulating glucose metabolism disorders and the development of innovative application scenarios.

To address this gap, we prepared maize starch-chlorogenic acid (EMS-CHA) complexes via extrusion processing and systematically evaluated their physicochemical properties and *in vitro* digestibility. Subsequently, we investigated their glycemic regulatory effects in diabetic rats by conducting comprehensive analyses including oral glucose tolerance tests and insulin resistance assessment. This study not only elucidated the *in vivo* mechanisms by which extruded starch-CHA complexes regulated blood glucose homeostasis but also provided a theoretical foundation for developing phenolic acid-fortified starch foods with enhanced health benefits.

2. Materials and methods

2.1 Materials

Maize starch (Food grade, purity 98%) was bought from Hua Lu foodstuff development Co. Ltd (Suzhou). Invertase (CAS:9001-57-4, from baker's yeast, ≥300 U/mg) and porcine pancreatic α-amylase (CAS: BIO-000003, ≥10 U/mg) were purchased from Sigma-Aldrich Chemical Co. (Milwaukee, WI, USA), and α-amyloglucosidase (CAS: 9032-08-0, 106 U/mL) were bought from Aladdin Co. (Shanghai, China). Chlorogenic acid (CAS: 2450-53-5, purity ≥ 98%) purchased from Nanjing Herbal Source Biotechnology Co.,

LTD. A glucose assay kit (GOPOD) was obtained from Megazyme International Ireland (Bray Business, Park, Bray, Co. Wicklow, Ireland). FINS (ZC-54525) were purchased from Shanghai ZCIBIO Biotechnology Co., LTD. was bought from Abcam (Shanghai). All the organic reagents involved in the experiment analytically pure.

2.2 Preparation of EMS-CHA complexes

EMS-CHA complexes were prepared according to our previous study [15]. Briefly, maize starch (MS, 1000 g, dry weight) was mixed with chlorogenic acid at different proportion (0.0, 0.5%, 1.0%, 1.5% and 2.0% (w/w), based on dry weight of maize starch), respectively. The moisture of the mixture was adjusted to 30% (w/w) with distilled water, followed by equilibration at 4℃ for 24 h. After that, the mixture was extruded by two screw extrusion (TSE 27 EBYJ, Guangzhou Potop CO. LTD.). The heat zones temperature is 30℃, 50, 75℃, 85℃, 90℃ and 100℃, respectively, with a screw speed was 150 rpm. The extruded products were then lyophilized and ground into powder and pass through 200 mesh [15]. The sample were named EMS, EMS-0.5CHA, EMS-1.0CHA, EMS-1.5CHA and EMS-2.0CHA, respectively.

2.3 Combined amount of chlorogenic acid

The complexes (1 g) were mixed with 10 mL 80% (v/v) cooling acetone, thoroughly stirred with a magneton for 10 min, and then centrifuged at 5000 rpm for 5 min. The supernatant was collected, and the sediment was re-extracted twice following the same procedure. All supernatants were aggregated and centrifuged again at 5000 rpm for 5 min to obtain a clear solution. This solution was further concentrated at 50℃ and redissolved with 5 mL methanol (HPLC grade) [15].

Stock solutions of chlorogenic acid at concentrations of 0, 0.2, 0.4, 0.6, 0.8, 1.0 mg/mL were prepared with methanol (HPLC grade). All samples and the mobile phase were filtered through a 0.45 μm membrane prior to analysis. Qualitative analysis of chlorogenic acid was conducted with a Waters system with a UV-Vis detector (Waters e2698) according to Shen et al. (2018). A reverse phase column (ZORBAX SB-C18, 250 mm × 4.6 mm i.d., 5 μL) was used to analyze the quality of chlorogenic acid. Mobile phase solvents A and B were 0.1% (v/v) formic acid and methanol solution (HPLC grade), respectively. The injected volume was 10 μL, and the column temperature was maintained at 25℃. The solvent flow rate was 1.0 mL/min with the following linear elution gradient: 20% B (10 min), 20%-40% B (20 min), 40%-20% B (2 min) and 20% B (8 min). Chlorogenic acid was qualitatively determined by retention time [15]. The content of free chlorogenic acid calculated from the standard curve, while the bound amount of chlorogenic acid was calculated using the following formula (Eq. 1)

$$Combined\ \ amount\ \ (mg/g\ starch) = (\mathrm{Total} - \mathrm{Free})chlorogenic\ \ acid \quad (1)$$

2.4 Surface structure and gelatinized degree of EMS-CHA complexes

The surface structures of MS, mixture of maize starch and chlorogenic acid, EMS and EMS-CHA complexes were observed using a scanning electron microscope (Sigma 300, ZEISS, Germany), respectively.

The gelatinized degree (GD) of EMS and the complexes was analyzed following the method described in Kuo et al. with slight modification[16]. Briefly, 0.5 g ground sample was added to 24.5 mL distilled water and 0.5 mL 10 mol/L KOH solution, then thoroughly stirred with a magnet for 10 min. The resulting slurry was centrifuged at 5000 ×g for 10 min. A 0.5 mL supernatant was collected and mixed with 0.5 mL HCl (0.2 mol /L), 4 mL distilled water, and 50 μL iodine reagent. Finally, 50 μL of the reaction mixture was fully mixed with 200 μL of distilled water, and the absorbance was measured by a microplate reader (Thermo Fisher Scientific Oy Ratastie 2, Vantaa, Finland). The absorbance value defined as A_1.

The procedure was repeated with 23.75 mL of distilled water and 1.25 mL of KOH solution, with 0.2 mol/L HCl replaced by an equal volume of 0.5 mol/L HCl; The corresponding absorbance was defined as A_2. GD was calculated as the ratio A_1/A_2. All samples were analyzed in triplicate for each sample.

2.5 Long/short-range order of EMS-CHA complexes

The crystal type and long-range order of extruded maize starch with and without chlorogenic acid were investigated by an X-ray diffractometer (X'Pert3 Powder, PANalytical, Netherlands) following the method described by Zheng et al. [15].The instrument was operated at 40 kV and 200 mA. Diffractograms were obtained by scanning from 4 to 40° (2θ) at a rate of 4°/min and a step size of 0.02° under room temperature. The V-type crystallinity zone (V-zone) ratio was calculated according to the following equation (Eq. 2).

$$V-zone\ \ ratio\ \ (\%) = \frac{\mathrm{t}}{\mathrm{T}} \times 100 \qquad (2)$$

Where T represented the total areas of crystalline and amorphous phase, t represented the area of V-zone.

The short-range order of samples was determined using a Nicolet AVATAR370 (Thermo Nicolet Co., Waltham, USA) spectrometer referring to the protocol by Zheng et al.,[15]. In brief, 2 mg of sample was mixed with 150 mg of KBr and milled thoroughly to pressed into a thin tablet. And the spectra were recorded in the range of 4000~400 cm^{-1} at a resolution of 2 cm^{-1}. The collected data were analyzed by Omnic 8.0 software (Thermo Electron Co., Madison, WI, USA).

2.6 In vitro digestibility

The determination of RDS, SDS and RS in the mixtures and complexes was performed according Zheng et al. [15]. Briefly, 1.0 g of starch samples was mixed with 50.0 mL of sodium acetate buffer solution (pH=5.2, 0.1 mol/L) and fully gelatinized, and then cooled to 37°C. A 3 mL of enzymatical solution (containing 360 U α-amylase and 240U α-glucosidase) was added, and the mixture was incubated with stirring at 37°C for 120 min. At 0, 20 and 120 min 0.5 mL of digestive solution was collected and mixed with 2.5 mL ethanol, and then centrifuged (3000 rpm, 5 min). Subsequently, 0.1mL of the supernatant was mixed with 0.5 mL invertase solution (7.5 mg/mL), and the glucose hydrolyzed from starch was determined by GOPOD kit assay. The contents of RDS, SDS and RS were calculated by the following equations (3-5):

$$RDS=0.9\times(G20-G0) \qquad (3)$$

$$SDS=0.9\times(G120-G20) \qquad (4)$$

$$RS=TS-RDS-SDS \qquad (5)$$

Where, G0, G20 and G120 represent the glucose contents at 0, 20 and 120 min, TS mean total starch and 0.9 represent conversion factor.

2.7 Postprandial glucose response

All animal experiments in present study were approved by the Laboratory of Animal Welfare and Ethics Committee of Zhejiang University (Approval No.: ZJU20220246). All male C57BL/6J mice (SPF, 20 ± 2 g, 6 weeks old, Slaccas Animal Company in Shanghai) were housed in a sterile laboratory environment under a constant temperature (25 ± 2℃) and humidity (40%~60%).

The mice were given free access to drinking water and a standard chow diet. Following a one-week of acclimation period, the mice were randomly divided into 5 groups (n=8 per group) and fasting for 12~14 h. Prior to intervention, blood samples were collected via tail snip, and fasting blood glucose levels was measured using a blood glucose meter (ACCU-CHEK Performa, R OCHE, American). Subsequently, each group was administered an individual starch solution (100 mg/mL, MS, MS+2.0CHA, EMS, EMS-2.0CHA) via oral gavage at a dosage of 0.1 mL/10 g body weight. This corresponded to a chlorogenic acid dosage of approximately 0.2 mg/g body weight, which is considered a safe dose for mice. One additional group served as the control and was administered a glucose solution (200 mg/mL) via oral gavage at a dosage of 2 mg/g body weight. Blood glucose levels were collected at 0, 30, 60, 90 and 120 min post-gavage via tail snip and the area under curve (AUC) was calculated to evaluate postprandial glycemic responses. Additionally, the glycemic index (GI) was calculated according to the following formula:

$$GI = \frac{AUC_{Sample}}{AUC_{Glucose}} \times 100 \quad (6)$$

where ACU_{Sample} was 2 h after the digestion of the starchy sample, $ACU_{Glucose}$ was 2 h after the digestion of the glucose standard.

2.8 The effect of EMS-2.0CHA on diabetic rats

Male SD rats (150 ± 20 g, 6 weeks old) were purchased from Slyke and fed in the animal center of Zhejiang University (Ethics Approval No.: ZJU20220128). Following a 1-week acclimation period, the rats were randomly divided into 2 groups. One group (n=10) was fed a normal diet as the Control group, and the other group (n=50) was fed a high-fat diet, and this feeing regimen lasted for 6 weeks. After that, the rats fed with high-fat diet were weighed and intraperitoneally injected with streptozotocin (STZ) (1% (w/w)) at a dosage of 30 mg/kg body weight to induce diabetes mellitus (DM). After 72 h, rats with a fasting blood glucose level that higher than 11.1 mmol/L was considered successfully induced with DM. These DM rats were further divided into five subgroups: the DM rats fed with high-fat diet (HFD group, n=6), DM rats fed with a high-fat diet and received daily metformin at 150 mg/kg (Met group, n=6), DM rats fed with a high-fat diet which maize starch was replaced with EMS of equal quality (EMS group, n=6), DM rats fed with a high-fat diet and 2% (w/w) CHA (CHA group, n=6). DM rats fed with a high-fat diet in which maize starch was replaced with EMS-2.0CHA of equal quality (EMS-2.0CHA group, n=6). The Control group was fed with a normal diet without metformin, CHA, EMS or EMS-2.0CHA and lasted for 6 weeks.

The fasting blood glucose of all rats were collected at baseline (0), 2nd, 4th and 6th week. The insulin tolerance test (ITT) (0.5 U/kg of body weight) and oral glucose tolerance test (OGTT) (2 g/kg of body weight) were performed at the 5th and 6th week, respectively. After 6 weeks of intervention, all rats were euthanized by cervical dislocation. Blood samples were collected immediately and centrifuged at 3,000 ×g for 10 min at 4℃ to obtain plasma. For histological analysis, pancreas tissues were excised and fixed in 10% formalin.

2.9 Insulin level determination

Plasma insulin levels were determined by an ELISA kit from ZCBIO Biotechnology Company. Homeostasis model assessment-insulin resistance (HOMA-IR) and homeostasis model assessment-β (HOMA-β) were calculated according to the following equations (Eq. 7 and Eq. 8).

$$\text{HOMA-IR} = \text{FBG} \times \text{FINS} / 22.5 \quad (7)$$

$$\text{HOMA-}\beta = (20 \times \text{FINS}) / (\text{FBG} - 3.5) \quad (8)$$

Pancreatic insulin levels were determined by immunofluorescence (IF) staining with technical support from Wuhan Servicebio Technology. In brief, pancreatic tissues slices were subjected to antigen retrieval, followed by blocking with serum to reduce non-specific binding. The slices were first incubated with a primary antibody against insulin, then with the corresponding secondary antibody. Nuclei were counterstained with DAPI, and then self-fluorescence quencher was added. Subsequently, the slices were loaded with anti-fluorescence quench tablets and photographed under fluorescence microscope. For DAPI, the ultraviolet excitation wavelength ranges from 330~380 nm, with an emission wavelength of 420 nm (emitting blue fluorescence). For Cy3 (the fluorophore conjugated to the secondary antibody), the excitation wavelength is 510~560 nm, and the emission wavelength is 590 nm (emitting red fluorescence).

2.10 H&E stain

Pancreatic tissues soaked in 4% paraformaldehyde were rinsed with distilled water, then dehydrated for 30 min with gradient ethanol (50%, 70%, 80%, 95% and 100%). After dehydration, the tissues were cleared in xylene, embedded in paraffin, and sectioned into 5 μm-thick slices. The pancreatic sections were stained with hematoxylin for 5 min, rinsed with tap water for 4~6 s to remove excess stain, then counterstained with eosin for 2 min. Following staining, the sections were re-dehydrated through a graded ethanol series, cleared in xylene, and mounted with neutral balsam. The slides were cover slipped and air-dried at room temperature. Histopathological changes in the pancreatic tissues were observed under a light microscope, and images were captured at the corresponding magnification.

2.11 TdT-mediated dUTP Nick-End Labeling (TUNEL)

TUNEL assay was used to observe pancreatic cell apoptosis. When cells undergo apoptosis, some DNA endonucleases are activated. These endonucleases cut the genomic DNA between nucleosomes. When genomic DNA breaks, exposed 3'-OH can be catalyzed by Terminal Deoxynucleotidyl Transferase (TdT) to add fluorescein (fluorescein-DUTP) labeled with FITC. Thus, it can be detected through a fluorescence

microscope. This assay was also performed with technical support from Wuhan Servicebio Technology. The images were captured in white light and the apoptotic rate was calculated with the following equation (Eq.9):

$$Apoptotic\ rate\ (\%) = \frac{A_1}{A} \times 100 \qquad (9)$$

Where, A_1 and A represented the number of apoptotic cell and total cell in the area.

2.12 Statistical analysis

All data were expressed as mean ± standard deviation (SD), and all experiments conducted at least in triples. For animal experiments, the results were presented as mean ± standard error of the mean (SE). Statistical analysis was performed one-way analysis of variance (ANOVA) followed by Tukey's multiple comparation test. A statically significant difference was considered at $P < 0.05$ level.

3. Results and discussion

3.1. Morphology

As shown in Figure 1A, native maize starch exhibited a relatively smooth, spherical particles with diameters ranging from 10 to 30 μm. Microstructural analysis revealed distinct morphological alterations following extrusion processing: unlike the intact granular structure of MS, both extruded maize starch (EMS) and EMS-CHA complexes displayed irregular surfaces with complete loss of granular morphology, though only subtle differences were observed between EMS and EMS-CHA samples. This structural transformation was attributed to starch gelatinization under high temperature and pressure conditions of extrusion, with EMS achieving gelatinization degree of 85.54 ± 3.69%. Notably, the incorporation of CHA significantly reduced the gelatinization degree of EMS ($P < 0.05$, Table S1). This effect is likely due to competitive water-binding capacity of hydroxyl groups in CHA, which diminished the water availability required for the starch gelatinization [15].

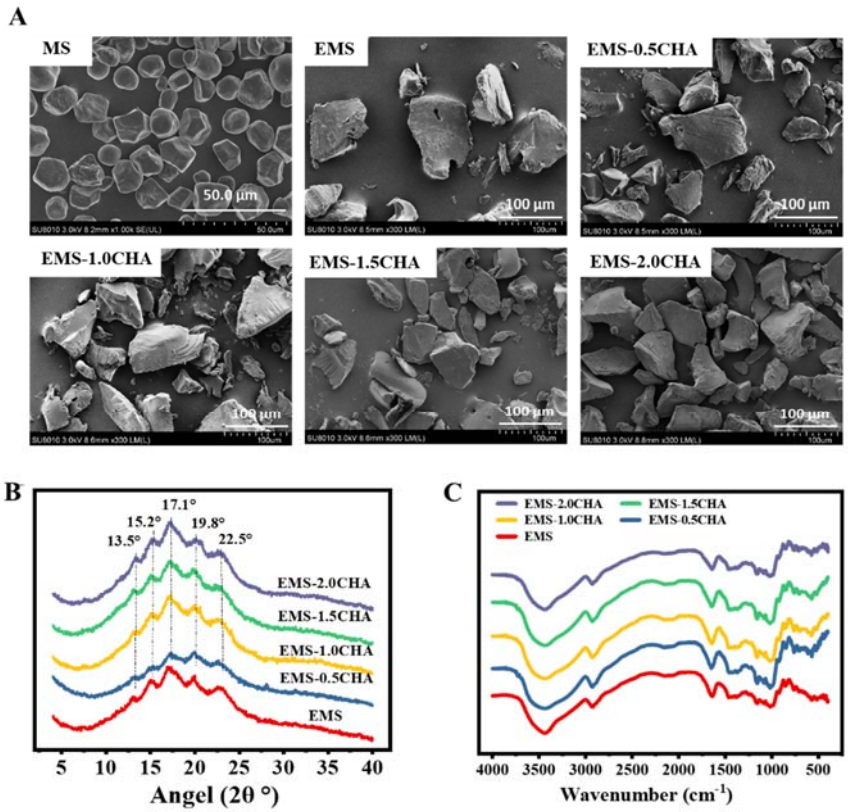

Figure 1 The SEM images of starches (A), scale bars were 50 μm and 100 μm (for different magnifications). The XRD patterns (B) and FT-IR spectra (C) of different starchy samples. Sample abbreviations: Native maize starch (MS), chlorogenic acid (CHA), extruded maize starch (EMS), EMS-0.5CHA, EMS-1.0CHA, EMS-1.5CHA and EMS-2.0CHA complexes referred to maize starch extruded with 0.5%, 1.0%, 1.5% and 2.0% (w/w) chlorogenic acid, respectively.

3.2 Characterization of EMS-CHA complexes

X-ray diffraction analysis revealed distinct structural transformations in the starch samples and complexes. Normal maize starch showed typical diffraction peaks at 15.0°, 17.1°, 18.1° and 22.5° (2θ), consistent with the typical peaks of A-type starch [17]. Following extrusion processing, both EMS and EMS-CHA complexes exhibited emerging diffraction peaks at 12.9° (2θ), accompanied by reduced peak intensity at 15.0° and 22.5° (2θ) and complete disappearance of the 18.1° (2θ) peak-confirming the successful transition to A+V-type crystallinity. With increasing chlorogenic acid addition, more obvious diffraction peaks at 12.9° and 19.8° (2θ) were observed. The relative crystallinity of the complexes increased to 20.13% (in EMS-2.0CHA), and the proportion of V-zone also increased from 14.94% to 18.43% (Table 1), indicating that chlorogenic acid could promote the formation V-type crystalline structure [18]. From comparison, the physical mixture of maize starch and chlorogenic acid exhibited the characteristic peaks of chlorogenic acid (Figure S1A and 1B), suggesting that no intermolecular interaction between maize starch in the physical mixture. Hot extrusion processing of maize starch induces two key changes in starch molecules: depolymerization and recrystallization. High temperature cleaves glycosidic bonds in starch chains, reducing molecular weight (a direct sign of depolymerization) as showed in Table S1. While extrusion melting destroys crystalline regions, subsequent cooling drives molecular chain rearrangement into ordered crystalline structures, increasing crystallinity (including V-zone ratio) and reflecting recrystallization in Table 1.

The combined amount of chlorogenic acid in the complexes was shown in Figure 2A. Over 90% chlorogenic acid was combined with maize starch following extrusion, with the highest combined amount (18.17 ± 0.11 mg/g) observed in the EMS-2.0CHA complexes. Extrusion processing induced the disassociation of the starch chains, which provided an opportunity for chlorogenic acid to combine with starch and form stable EMS-CHA complexes [19]. These findings aligned with previous reports on heat-induced polyphenols-starch interactions, where binding capacity increased proportionally with the amount of added polyphenols, reaching a max loading efficiency of 71% [20].

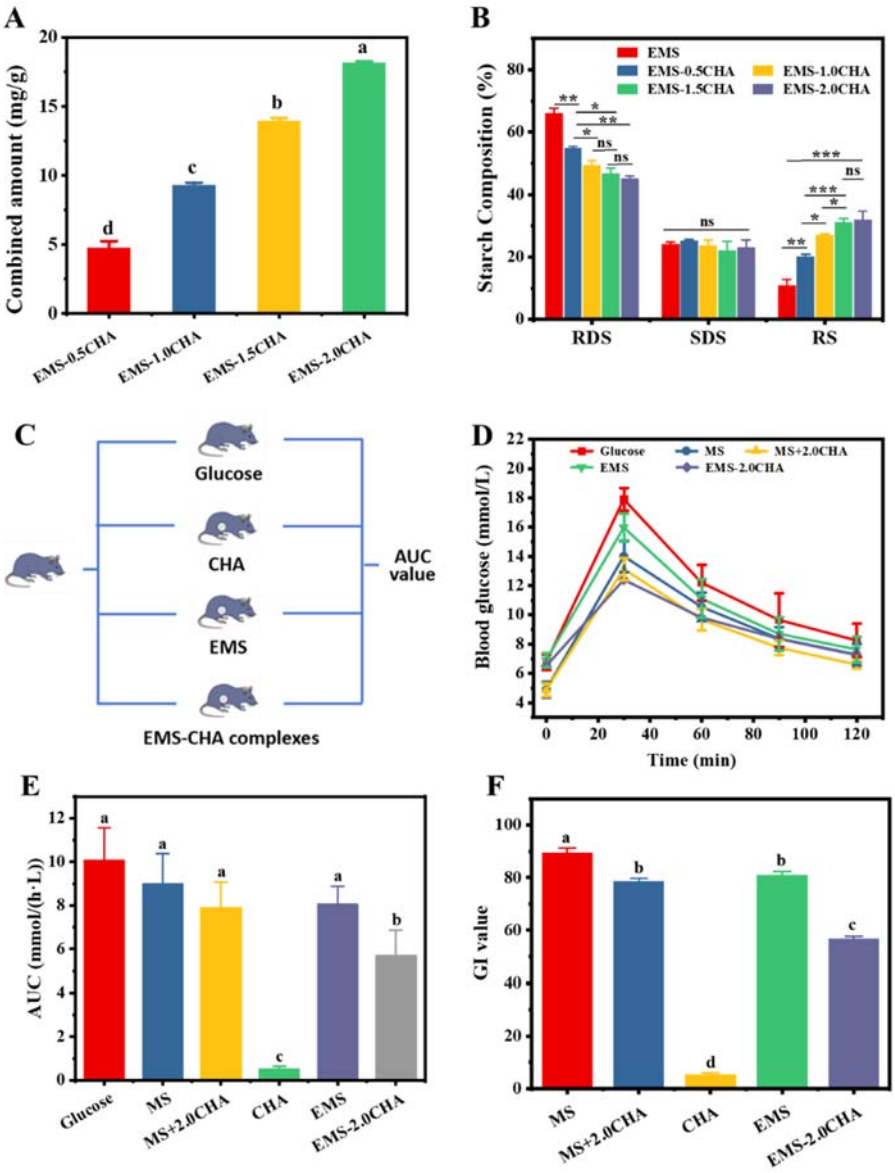

Figure 2 The combined amount of CHA (A); starchy fractions of samples(B). The experimental flow of postprandial glycemic response in health mice (C). The blood glucose response of rats after administration of starchy samples in health mice (D). The AUC values (E) and GI values (F) of starch sample. Sample abbreviations: Native maize starch (MS); extruded maize starch (EMS); EMS-0.5CHA, EMS-1.0CHA, EMS-1.5CHA, and EMS-2.0CHA complexes refer to extruded maize starch incorporated with 0.5%, 1.0%, 1.5%, and 2.0% (w/w) CHA, respectively.

Table 1 Crystallinity (%), V-zone ratio (%), $R_{1047/1022}$ and $R_{1022/995}$ of starchy samples

Samples	Crystallinity	V-zone ratio	$R_{1047/1022}$	$R_{1022/995}$
MS	32.18±1.26 ^{a}	16.32 ±0.99 ^{b}	1.182 ±0.02 ^{a}	0.896 ±0.05 ^{e}
EMS	18.77±1.30 ^{b}	14.94 ±1.10 ^{c}	1.004 ±0.06 ^{c}	0.997 ±0.02 ^{d}
EMS-0.5CHA	19.99±1.14 ^{b}	15.51 ±0.91 ^{bc}	0.971 ±0.03 ^{d}	1.033 ±0.03 ^{b}

EMS-1.0CHA	20.34±0.96 [b]	16.03 ±1.60 [ab]	0.942 ±0.01 [e]	1.068 ±0.04 [a]
EMS-1.5CHA	20.10±1.47 [b]	16.57 ±1.09 [ab]	1.017 ±0.02 [b]	1.014 ±0.06 [c]
EMS-2.0CHA	20.13±1.06 [b]	18.43 ±0.91 [a]	1.003 ±0.04 [c]	0.997 ±0.07 [d]

Note: Different lowercase letters indicate significant differences ($P < 0.05$) among different groups

FT-IR analysis (Figures 1C) revealed no new absorption peaks in either the physical mixture of maize starch and chlorogenic acid or the EMS-CHA complexes compared to native maize starch. This indicated that the interaction between MS and CHA was primarily mediated through noncovalent forces. In addition, the broad absorption band between 3000~3600 cm^{-1} was related to in the intramolecular or intermolecular hydrogen bonds (C-H stretching region) of the hydroxyl groups in starch [21]. Notably, the bandwidth of this band reflected the strength of hydrogen bonding interactions. There was no significant change in the C-H band width of the maize starch under physical mixing, indicating that the chlorogenic acid did not affect the intrinsic hydrogen bonds within the maize starch molecules under physical mixing conditions. However, extrusion processing induced marked changes: with increasing chlorogenic acid concentration, the C-H band gradually broadened. This clearly demonstrated the formation of new hydrogen bonds between chlorogenic acid and maize starch during extrusion process.

$R_{1047/1022}$ or $R_{1022/995}$ was used to evaluate the short-range order of starch. A higher $R_{1047/1022}$ value and a lower $R_{1022/995}$ value indicated a higher degree of short-range order of starch [21]. As shown in Table 1, native maize starch had highest $R_{1047/1022}$ value and a lower $R_{1022/995}$ value among all samples ($p< 0.05$). Extrusion treatment significantly decreased $R_{1047/1022}$ value and increased $R_{1022/995}$ value, suggesting that extruded treatment disrupted the short-range order of maize starch. This effect may be attributed to enhanced internal molecular motion of MS under high temperature and high pressure, which destroyed its original short-range ordered structure [22]. In addition, chlorogenic acid had no significant effect on the $R_{1047/1022}$ or $R_{1022/995}$ value of maize starch-chlorogenic acid complexes, indicating that chlorogenic acid did not alter the short-range order of extruded maize starch.

3.3 Digestive properties

The contents of RDS, SDS and RS in MS, EMS, and EMS-CHA complexes were presented in Figure 2B. MS exhibited a RDS content of 72.89 ± 1.39%, which decreased to 66.10 ± 1.60% following extrusion (i.e., in EMS). This reduction may be attributed the retrogradation of maize starch during cooling stage post-extrusion, which increases the difficulty of enzymatic hydrolysis. The addition of chlorogenic acid further modulated starch digestibility: in the EMS-2.0CHA complexes, the content of RDS was significantly reduced to 45.08 ± 0.90%, while the RS content was elevated to 31.98 ± 2.63%. These findings aligned with previous reports by Guo et al. [23] and confirmed that the EMS-2.0CHA complex possesses superior starch digestion-retarding properties compared extruded maize starch alone.

The postprandial glycemic response in healthy mice was evaluated following administration of different starch samples (Figure 2C). As shown in Figure 2D, MS exhibited an AUC value of 9.73 ± 1.35 mmol/h·L. While the physical mixture with 2.0% (w/w) CHA reduced the AUC to 8.42 ± 1.17 mmol/h·L, this decrease was not statistically significant ($p \geq 0.05$). In contrast, EMS alone showed a lower AUC (8.17 ± 0.81

mmol/h·L), and the EMS-2.0CHA complex further significantly reduced the AUC to 5.72 ± 1.13 mmol/h·L. These results demonstrated that CHA exerted a significant hypoglycemic effect when combined with maize starch via extrusion processing. This effect was likely due to the formation of V-type crystalline structures and increased RS content in EMS-2.0CHA (Figure 3). Our findings were consistent with previous reports on polyphenol-starch interactions: Apple polyphenols (rich in CHA) have been shown to attenuate postprandial glucose and insulin responses in mice [24], and tea polyphenols not only reduced peak blood glucose levels but also delay the time to peak glucose concentration (60 min) in murine models [25]. These collective observations underscored the potential of polyphenol-starch complexes in modulating glycemic responses.

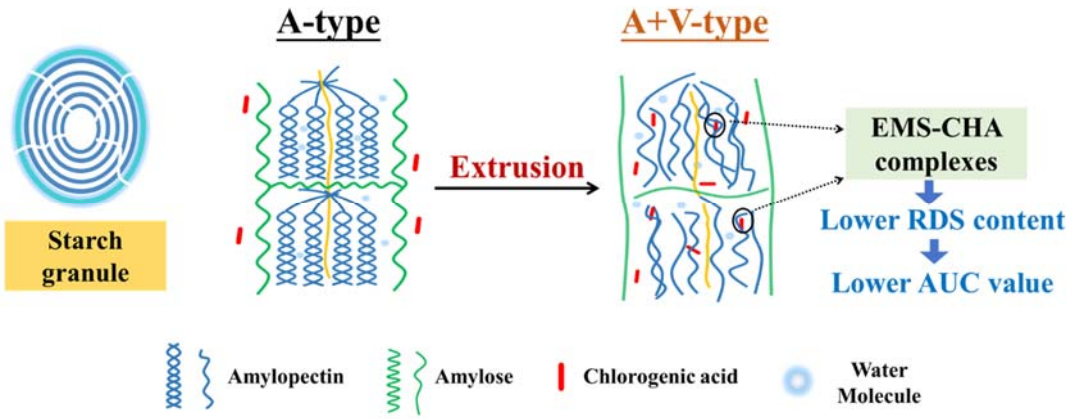

Figure 3 Potential mechanism underlying the delay of postprandial blood glucose elevation by EMS-CHA complexes

3.4 The fasting blood glucose level and OGTT

Based on its superior RS content, enhanced chlorogenic acid binding capacity, and reduced glycemic response (AUC), the EMS-2.0CHA complex was selected to evaluate its blood glucose regulatory effects in DM rats. Following a 6-week dietary intervention (Figure 4A), significant differences in fasting blood glucose control were observed among the groups. While the HFD group exhibited elevated fasting blood glucose levels (18.68 ± 2.40 mmol/L), all treatment groups showed significant reductions: Met group (8.76 ± 1.29 mmol/L), EMS group (11.57 ± 2.27 mmol/L), and EMS-2.0CHA group (11.75 ± 2.75 mmol/L) (p<0.05) (Table 2). These results demonstrated that both EMS and EMS-2.0CHA complex possessed significant hypoglycemic effects, which were comparable to metformin in DM rats.

Table 2 FBG (mmol/L) and AUC (mmol/(h·L)) of rats (n=6)

Groups	FBG		AUC（OGTT）	AUC'（ITT）
	0	6th week		
Control	5.09±0.59^{a}	4.64±0.30^{a}	6.45±2.04^{a}	3.64±1.29^{a}
HFD	15.14±3.75^{b}	18.69±2.40^{d}	21.34±2.44^{c}	9.32±2.87^{b}
Met	15.45±4.34^{b}	8.76±1.29^{bc}	15.98±2.54^{b}	17.10±1.97^{d}
EMS	15.58±3.33^{b}	11.57±2.27^{bc}	15.71±4.82^{bc}	12.40±2.28^{bc}
CHA	15.74±2.56^{b}	11.85±2.12^{c}	15.98±2.99^{b}	12.78±1.07^{bc}
EMS-2.0CHA	16.24±2.62^{b}	11.75±2.75^{bc}	15.15±2.63^{b}	15.30±0.95^{d}

Note: Different lowercase letters indicate significant differences (P < 0.05) among different groups

Figure 4B and Table 2 showed the OGTT and AUC results of rats at the 6th week. Following intragastric administration of 2 g/kg glucose solution, the Control group exhibited stable blood glucose fluctuations: blood

glucose peaked at 30 min (10.49 ± 1.89 mmol/L) and returned to the normal level within 2 h (5.77 ± 0.80 mmol/L), with AUC value of 6.45 ± 2.04 mmol/h·L. In contrast, the HFD group showed poor blood glucose tolerance, with blood glucose reaching 33.13 ± 0.31 mmol/L after glucose gavage and the AUC value of 21.34 ± 2.44 mmol/h·L. For DM rats in the Met group and EMS-2.0CHA group, the AUC values were 15.18 ± 2.54 and 15.15 ± 2.63 mmol/h·L, respectively-both significantly than that of the HFD group ($P < 0.05$). These findings demonstrated that EMS-2.0CHA complex supplementation effectively mitigates postprandial glycemic excursions in DM rats, with comparable efficacy to metformin treatment.

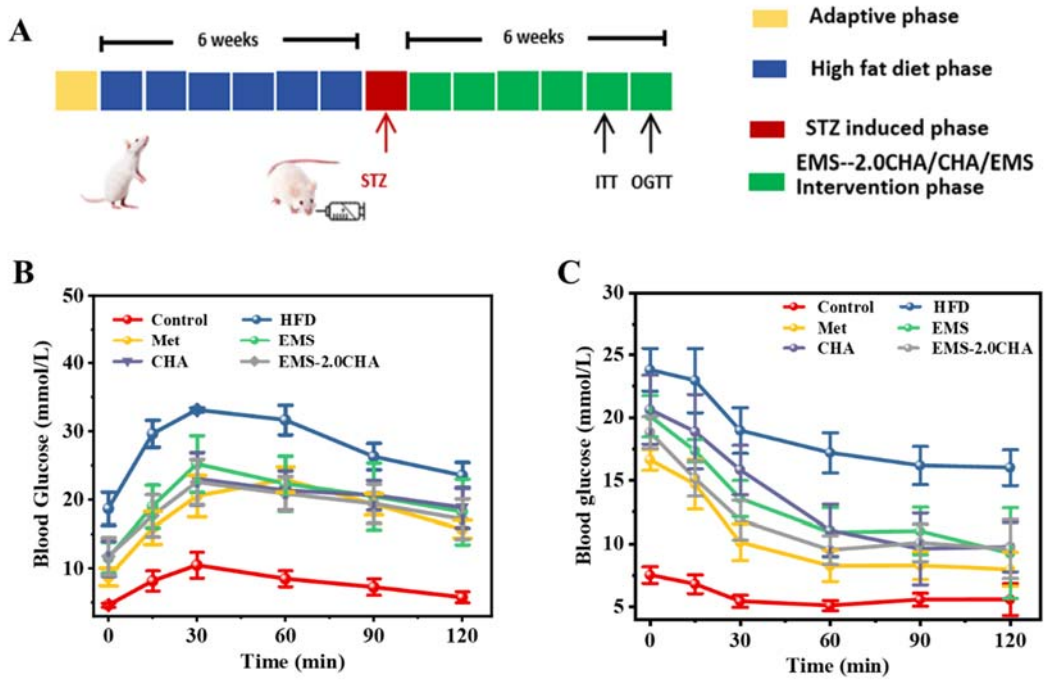

Figure 4 The experimental scheme of dietary intervention in diabetic rats (A). The blood glucose levels during the oral glucose tolerance test (B) and insulin tolerance test (C) in different groups. Normal diet (Control), high-fat diet (HFD), native maize starch (MS), chlorogenic acid (CHA), extruded maize starch (EMS), maize starch extruded with 2.0% (w/w) chlorogenic acid (EMS-2.0CHA).

3.5 EMS-2.0CHA improved the insulin levels

Following intraperitoneal injection of 0.5 U/kg insulin, blood glucose levels in the Control group decreased and returned to baseline within 60 min (Figure 4C). The area on the curve (AUC') of the HFD group was 9.32 ± 2.87 mmol/h·L. Notably, both EMS and EMS-2.0CHA groups of rats exhibited significantly elevated AUC' value ($P < 0.05$) (Table 2), suggesting enhanced cellular glucose uptake and utilization in response to insulin stimulation [26]. These findings indicated that dietary intervention with EMS and EMS-2.0CHA complex improved insulin sensitivity in the treated animals, facilitating more efficient glucose clearance and better maintenance of blood glucose homeostasis [27].

Figure 4C presented the insulin distribution patterns in pancreatic islets across experimental groups. In the Control group, insulin exhibited uniform distribution and strong fluorescence intensity, reflecting normal pancreatic β-cell function and insulin secretion for glucose metabolism regulation [28]. The HFD group showed markedly diminished fluorescence intensity, which resulted from combined effects of STZ-induced

β-cell destruction and high-fat diet-induced insulin resistance. Metformin treatment (150 mg/kg) significantly restored islet morphology and function, as evidenced by enhanced fluorescence intensity and wider insulin distribution in the Met group. Notably, EMS-2.0CHA complex supplementation similarly improved insulin production capacity, with fluorescence parameters significantly higher than those in the HFD group ($P < 0.05$). These morphological observations were corroborated by measurements of serum insulin level (Table 3). The Control group maintained insulin levels approximately three-fold higher than those in the HFD group. Both EMS and EMS-2.0CHA complex dietary interventions significantly elevated serum insulin concentrations compared with the HFD group ($P < 0.05$), confirming that dietary supplementation with EMS-2.0CHA complex effectively enhanced insulin secretion in diabetic rats.

3.6 EMS-2.0CHA alleviated insulin resistance

Traditionally, pancreatic islet β-cells have been recognized as primary regulators of glycemia. Diabetes mellitus occurred when severe insulin deficiency arises-due to islet cell destruction (type I diabetes) or peripheral tissue insulin resistance (type II diabetes) [26]. The normal biology and function of β-cells, including their insulin signaling, proliferation, and apoptosis, were important to maintain blood glucose homeostasis [29].

Table 3 Insulin level (mIU/L), HOMA-IR and HOMA-β values of rats

Groups	Insulin level	HOMA-IR	HOMA-β
Control	14.25±2.46^{c}	2.70±0.55^{a}	203.67±56.49^{d}
HFD	4.28±1.08^{a}	19.45±3.63^{c}	21.39±3.41^{a}
Met	8.68±1.18^{b}	3.36±0.59^{bc}	62.01±16.51^{c}
EMS	5.24±1.27^{a}	2.70±0.59^{a}	37.23±9.81^{b}
CHA	6.11±1.14^{ab}	3.00±0.34^{a}	40.52±6.09^{b}
EMS-2.0CHA	8.44±1.12^{b}	3.62±0.97^{bc}	50.78±15.58^{bc}

Note: Different lowercase letters indicate significant differences ($P < 0.05$) among different groups

HOMA-IR is a key index for assessing individual insulin resistance levels. It is calculated based on fasting blood glucose values and fasting insulin values, with higher HOMA-IR values indicating more pronounced insulin resistance. As shown in Table 4, the HFD group exhibited an 8-fold elevation in HOMA-IR and a 10-fold increase in HOMA-β compared to the Control group, demonstrating severe insulin resistance and impaired insulin secretion. Following 6 weeks of EMS-2.0CHA complex intervention, diabetic rats showed a significant reduction in HOMA-IR ($P < 0.05$) and a significant increase in HOMA-β ($P < 0.05$), indicating improved insulin sensitivity and β-cell function. Although these values did not fully normalize to Control group levels, the results were consistent with the outcomes of insulin assay.

3.6.1 HE staining of pancreatic tissue

HE staining of pancreatic tissue (Figure 6A) revealed distinct morphological differences among the experimental groups. In the Control group, islet cells were oval shape, uniformly distributed, and had abundant cytoplasm, indicating normal pancreatic architecture. In contrast, the HFD group displayed significant islet cells atrophy, along with irregular morphology and reduced cell numbers, consistent with

STZ-induced β-cell destruction [30]. The Met group showed partial recovery, characterized by increased islet cell size and quantity, albeit with persistent morphological irregularities. Notably, both the EMS and EMS-2.0CHA groups displayed marked improvements in islet cell morphology, volume, and number compared to the HFD group. The EMS-2.0CHA treatment exhibited the most pronounced restorative effect, suggesting enhanced islet cell repair capacity. These observations are consistent with prior studies indicating that chlorogenic acid and metformin alleviated pancreatic damage in diabetic rats [30]. Furthermore, insulin immunofluorescence results supported the hypothesis that EMS-2.0CHA promotes islet cell regeneration, thereby reducing insulin resistance (Table 3, Figure 5) and enhancing insulin secretion to improve glycemic control. This effect was likely mediated by the synergistic effects of chlorogenic acid and RS in the formulation.

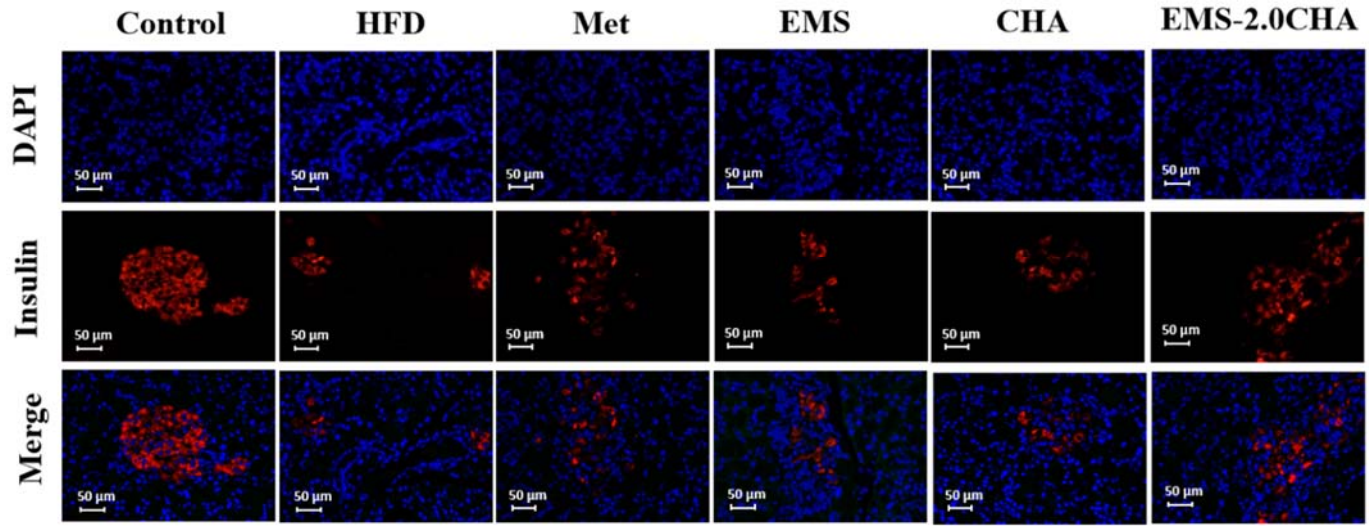

Figure 5 Immunofluorescence staining of insulin in pancreatic tissue, the red and blue represented insulin and nuclear, respectively, scale bars were 50 μm.

3.6.2 Apoptosis of islet cells

The apoptotic rate of islet cells was calculated via image analysis as the ratio of apoptotic cells to total islet cells in the observation field. In normal pancreatic tissue, hematoxylin-stained nuclei appeared blue, while DAB-stained apoptotic nuclei exhibited a characteristic brown-yellow coloration. Compared to the Control group, the HFD group displayed extensive islet cell damage-evidenced by a significant increase in brown-yellow staining (Figure 6B), particularly in β-cells-and a marked elevated in apoptotic rate (Table S2).

Among the treatment groups, the EMS-2.0CHA group had the lowest apoptotic rate, (second only to the Control group), indicating its potent protective effect against islet cell injury and apoptosis. This protective effects was likely mediated by the increased RS content and the incorporation of chlorogenic acid in the modified extruded maize starch, which collectively attenuated pancreatic cell apoptosis [31, 30].

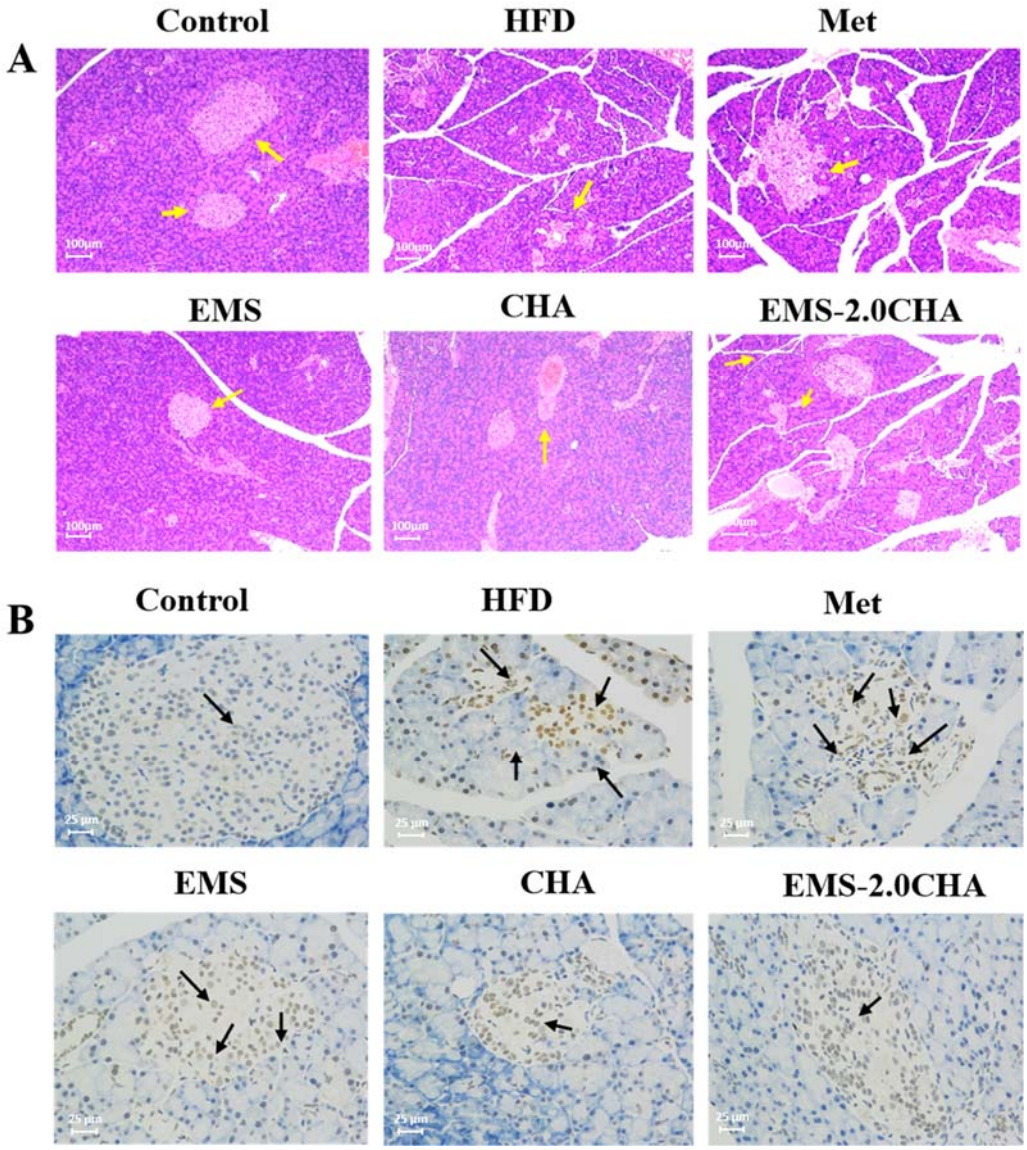

Figure 6 H&E staining of pancreas in different groups (A), scale bars were 100 μm. Pancreas cell apoptosis detected by immunofluorescence staining in different groups (B), scale bars were 25 μm.

As illustrated in Figure 7, DM rats fed a high-fat diet exhibited severe glucose regulation impairment, aligned with pancreatic damage-characterized by reduced β-cell mass and elevated insulin resistance-ultimately leading to increased pancreatic apoptosis. EMS-2.0CHA complex formulated with a higher proportion of RS and bound chlorogenic acid, exerted superior efficacy compared to native maize starch, as evidenced by the lowest AUC value in glucose tolerance tests. Moreover, EMS-2.0CHA complex significantly alleviated hyperglycemia and restored blood glucose homeostasis in DM rats. This effect was mediated by reduced pancreatic cell apoptosis, improved β-cell survival, and enhanced functional recovery of pancreatic islets- collectively enabling more effective glucose regulation. These findings offered novel insights into the mechanism by which EMS-2.0CHA complex modulated glucose metabolism through the preservation of pancreatic function. The synergistic interaction between chlorogenic acid and RS was critical; however, further research is required to: Elucidate the direct impact of this synergy on blood glucose control and investigate the potential involvement of gut microbiota in mediating these effects.

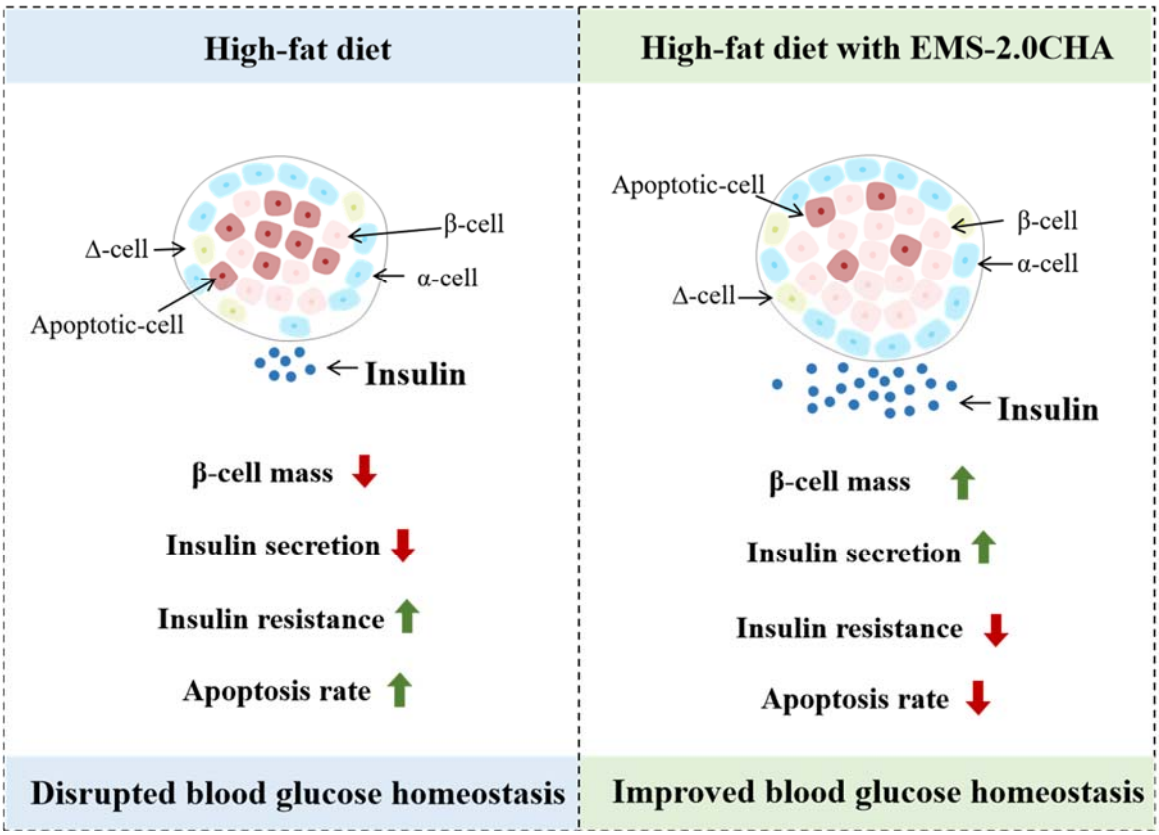

Figure 7 The potential effect of EMS-2.0CHA complex on the regulation of blood glucose homeostasis.

4. Conclusion

This study demonstrated that maize starch extruded with 2.0% (w/w) chlorogenic acid (EMS-2.0CHA) complex exhibited significant changes in its digestibility profile, characterized by reduced RDS content and increased SDS and RS fractions. These structural modifications correlated with a lower AUC value in health mice following consumption of EMS-2.0CHA complex. Furthermore, we also confirmed that EMS-2.0CHA complex improved fasting blood glucose levels and glucose tolerance in diabetic rats. It also significantly enhanced paracrine functions, such as insulin sensitivity and insulin levels during the oral glucose tolerance, thereby ameliorating glucose intolerance and reducing insulin resistance. The therapeutic potential of EMS-2.0CHA was supported by these findings. Our results provided a novel approach for the development of functional food ingredients that integrate phytochemicals with modified starches to address glucose metabolism disorders.

Declaration of competing Interests

The authors declare no competing financial interest.

Funding

This work was supported by the National Natural Science Foundation of China (31901616), National Natural Science Foundation of Zhejiang Province (LY22C200007) and National Natural Science Foundation of Ningxia Province (2022A0140), Research start-up foundation of Fuzhou University (XRC-24047; 511422); Fuzhou University Testing Fund of precious apparatus (2025T035).

References

[1] W. Liang, Y. Lan, C. Chen, M. Song, J. Xiao, Q. Huang, Y. Cao, C. Ho, M. Lu, Modulating effects of capsaicin on glucose homeostasis and the underlying mechanism, *Crit. Rev. Food. Sci. Nutr.* (2021) 1-19, https://doi.org/10.1080/10408398.2021.1991883.

[2] J.E. Campbell, C.B. Newgard, Mechanisms controlling pancreatic islet cell function in insulin secretion, Nat. *Rev. Mol. Cell Biol.* 22 (2) (2021) 142-158, https://doi.org/10.1038/s41580-020-00317-7.

[3] H. Steinbrenner, L.H. Duntas, M.P. Rayman, The role of selenium in type-2 diabetes mellitus and its metabolic comorbidities, *Redox Biol.* 50 (2022) 102236, https://doi.org/10.1016/j.redox.2022.102236.

[4] J. Su, J. Xu, S. Hu, H. Ye, L. Xie, S. Ouyang, Advances in small-molecule insulin secretagogues for diabetes treatment, *Biomed. Pharmacother.* 178 (2024) 117179, https://doi.org/10.1016/j.biopha.2024.117179.

[5] Y. Fu, E. Jiang, Y. Yao, New techniques in structural tailoring of starch functionality, *Annu. Rev. Food Sci. Technol*. 13 (1) (2022) 117-143, https://doi.org/10.1146/annurev-food-102821-035457.

[6] D. Yang, Q. Guo, R. Li, L. Chen, B. Zheng, Amylose content controls the v-type structural formation and *in vitro* digestibility of maize starch-resveratrol complexes and their effect on human gut microbiota, *Carbohydr. Polym*. 327 (2024) 121702, https://doi.org/10.1016/j.carbpol.2023.121702.

[7] P.J. Butterworth, B.H. Bajka, C.H. Edwards, F.J. Warren, P.R. Ellis, Enzyme kinetic approach for mechanistic insight and predictions of *in vivo* starch digestibility and the glycaemic index of foods, *Trends Food Sci. Technol.* 120 (2022) 254-264, https://doi.org/10.1016/j.tifs.2021.11.015.

[8] X. Lu, R. Ma, J. Zhan, F. Wang, Y. Tian, The role of protein and its hydrolysates in regulating the digestive properties of starch: a review, *Trends Food Sci. Technol.* 125 (2022) 54-65, https://doi.org/10.1016/j.tifs.2022.04.027.

[9] J. Guo, L. Tan, L. Kong, Impact of dietary intake of resistant starch on obesity and associated metabolic profiles in human: a systematic review of the literature, *Crit. Rev. Food. Sci. Nutr.* (2020) 1-17, https://doi.org/10.1080/10408398.2020.1747391.

[10] M. Cai, J. Feng, J. Wang, P. Chen, Z. Ge, W. Liu, P. Sun, L. Wu, J. Wu, Characterization of various noncovalent polyphenol–starch complexes and their prebiotic activities during *in vitro* digestion and fermentation, J. Agric. *Food. Chem.* 72 (4) (2024) 2250-2262, https://doi.org/10.1021/acs.jafc.3c09327.

[11] J. Yang, M. Dong, F. Fang, Y. Li, C. Li, Effects of varied preparation processes on polyphenol-rice starch complexes, *in vitro* starch digestion, and polyphenols release, *Food Chem*. 450 (2024) 139330. https://doi.org/10.1016/j.foodchem.2024.139330

[12] J. Huo, L. Wang, J. Ma, X. Yue, K. Wang, X. Ma, X. Yu, Z. Xiao, Different effects of polyphenols on hydration, pasting and rheological properties of rice starch under extrusion condition: From the alterations in starch structure, *Food Chem*. 464 (2025) 142002. https://doi.org/10.1016/j.foodchem.2024.142002

[13] Y. Zheng, J. Tian, W. Yang, S. Chen, D. Liu, H. Fang, H. Zhang, X. Ye, Inhibition mechanism of ferulic acid against α-amylase and α-glucosidase, *Food Chem.* 317 (2020) 126346, https://doi.org/10.1016/j.foodchem.2020.126346.

[14] M. Shahwan, F. Alhumaydhi, G.M. Ashraf, P.M.Z. Hasan, A. Shamsi, Role of polyphenols in combating type 2 diabetes and insulin resistance, *Int. J. Biol. Macromol.* 206 (2022) 567-579, https://doi.org/10.1016/j.ijbiomac.2022.03.004.

[15] Y. Zheng, X. Yin, X. Kong, S. Chen, E. Xu, D. Liu, Y. Ogawa, X. Ye, J. Tian, Introduction of chlorogenic acid during extrusion affects the physicochemical properties and enzymatic hydrolysis of rice flour, *Food Hydrocoll.* 116 (2021) 106652, https://doi.org/10.1016/j.foodhyd.2021.106652.

[16] C. Kuo, C. Shieh, S. Huang, H. David Wang, C. Huang, The effect of extrusion puffing on the physicochemical properties of brown rice used for saccharification and chinese rice wine fermentation, *Food Hydrocoll.* 94 (2019) 363-370, https://doi.org/10.1016/j.foodhyd.2019.03.040.

[17] Y. Zheng, J. Tian, X. Kong, W. Yang, X. Yin, E. Xu, S. Chen, D. Liu, X. Ye, Physicochemical and digestibility characterisation of maize starch–caffeic acid complexes, *LWT* 121 (2020) 108857, https://doi.org/10.1016/j.lwt.2019.108857.

[18] X. Zhou, Y. Xing, T. Meng, J. Li, Q. Chang, J. Zhao, Z. Jin, Preparation of v-type cold water-swelling starch by ethanolic extrusion, *Carbohydr. Polym.* 271 (2021) 118400, https://doi.org/10.1016/j.carbpol.2021.118400.

[19] Y. Yang, J. Liu, X. Wang, J. Deng, H. Jiang, Effects of different polyphenols on the structural, physicochemical, digestive and 3D printing properties of mashed potatoes, *Food Chem.* 488 (2025) 144919. https://doi.org/10.1016/j.foodchem.2025.144919

[20] Z. Zhang, J. Tian, H. Fang, H. Zhang, X. Kong, D. Wu, J. Zheng, D. Liu, X. Ye, S. Chen, Physicochemical and digestion properties of potato starch were modified by complexing with grape seed proanthocyanidins, *Molecules* 25 (5) (2020) 1123, https://doi.org/10.3390/molecules25051123.

[21] W. Yang, X. Kong, Y. Zheng, W. Sun, S. Chen, D. Liu, H. Zhang, H. Fang, J. Tian, X. Ye, Controlled ultrasound treatments modify the morphology and physical properties of rice starch rather than the fine structure, *Ultrason. Sonochem.* 59 (2019) 104709, https://doi.org/10.1016/j.ultsonch.2019.104709.

[22] J. Ye, X. Hu, S. Luo, W. Liu, J. Chen, Z. Zeng, C. Liu, Properties of starch after extrusion: a review, *Starch - Stärke* 70 (11-12) (2018) 1700110, https://doi.org/10.1002/star.201700110.

[23] L. Liu, S. Lei, X. Lin, D. Bodjrenou, Y. Zhang, B. Zheng, H. Liang, Synergistic regulation of colon microflora and metabolic environment by resistant starch and sodium lactate in hyperlipidemic rats, *International Journal of Biological Macromolecules*. 307 (2025) 141933, https://doi.org/10.1016/j.ijbiomac.2025.141933.

J. Guo, L. Tan, L. Kong, Impact of dietary intake of resistant starch on obesity and associated metabolic profiles in human: a systematic review of the literature, *Crit. Rev. Food. Sci. Nutr.* 61 (6) (2021) 889-905, https://doi.org/10.1080/10408398.2020.1747391.

[24] D. Li, L. Sun, Y. Yang, Z. Wang, X. Yang, T. Zhao, T. Gong, L. Zou, Y. Guo, Young apple polyphenols postpone starch digestion *in vitro* and *in vivo*, *J. Funct. Foods* 56 (2019) 127-135, https://doi.org/10.1016/j.jff.2019.03.009.

[25] J. Liu, Y. Lv, J. Pan, Y. Jiang, Y. Zhu, S. Zhang, Effects of tea polyphenols and egcg on glucose metabolism and intestinal flora in diabetic mice fed a cornstarch-based functional diet, *Food Sci. Technol.* 42 (2022), https://doi.org/10.1590/fst.50821.

[26] L. Norton, C. Shannon, A. Gastaldelli, R.A. Defronzo, Insulin: the master regulator of glucose metabolism, *Metabolism.* 129 (2022) 155142, https://doi.org/10.1016/j.metabol.2022.155142.

[27] S. Virtue, A. Vidal-Puig, Gtts and itts in mice: simple tests, complex answers, *Nat. Metab.* 3 (7) (2021) 883-886, https://doi.org/10.1038/s42255-021-00414-7.

[28] E.C. Lien, H.M. Vander, Pancreatic beta cells put the glutamine engine in reverse, *Cell Metab.* 33 (4) (2021) 702-704, https://doi.org/10.1016/j.cmet.2021.03.010.

[29] C. Jain, S. Bilekova, H. Lickert, Targeting pancreatic β cells for diabetes treatment, *Nat. Metab.* 4 (9) (2022) 1097-1108, https://doi.org/10.1038/s42255-022-00618-5.

[30] B.L. Furman, Streptozotocin-induced diabetic models in mice and rats, *Current Protocols* 1 (4) (2021), https://doi.org/10.1002/cpz1.78.

[31] M.J. Keenan, J. Zhou, M. Hegsted, C. Pelkman, H.A. Durham, D.B. Coulon, R.J. Martin, Role of resistant starch in improving gut health, adiposity, and insulin resistance, *Adv. Nutr.* 6 (2) (2015) 198-205, https://doi.org/10.3945/an.114.007419.